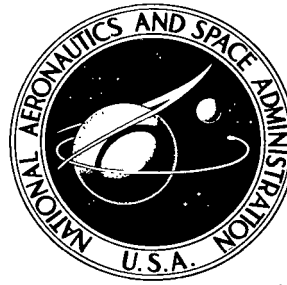


NASA TECHNICAL NOTE



NASA TN D-5193

e. 1

LOAN COPY: RETURN TO
AFWL (WLIL-2)
KIRTLAND AFB, N MEX



TECH LIBRARY KAFB, NM

NASA TN D-5193

NEWTONIAN AERODYNAMICS
FOR CIRCULAR CONES
MODIFIED TO PRODUCE LIFT
AT ZERO ANGLE OF ATTACK

by Barbara J. Short
Ames Research Center
Moffett Field, Calif.



NEWTONIAN AERODYNAMICS FOR CIRCULAR CONES MODIFIED
TO PRODUCE LIFT AT ZERO ANGLE OF ATTACK

By Barbara J. Short

Ames Research Center
Moffett Field, Calif.

NATIONAL AERONAUTICS AND SPACE ADMINISTRATION

For sale by the Clearinghouse for Federal Scientific and Technical Information
Springfield, Virginia 22151 - CFSTI price \$3.00

NEWTONIAN AERODYNAMICS FOR CIRCULAR CONES MODIFIED

TO PRODUCE LIFT AT ZERO ANGLE OF ATTACK

By Barbara J. Short

Ames Research Center

SUMMARY

A parametric study was conducted to determine the theoretical aerodynamic characteristics of right circular cones modified to produce lift at zero angle of attack. In the modification, portions of the cone lying above and behind an inclined plane surface were removed. Newtonian impact theory was used to express force and moment coefficients as functions of the manner in which the cone is terminated by this cutting plane at the base. In addition, relationships were formed that allow limits of acceptable design and performance characteristics to be imposed, such as lower limits of useful volume and lift-drag ratios, assurance of maintaining supersonic flow over the trailing edges, and the permissible range of center-of-gravity locations to assure trim at zero angle of incidence. The configurations studied suggest that it is practical to trim cones at a useful level of lift-drag ratio without inclining the axis of the basic cone relative to the airstream.

INTRODUCTION

Vehicles returning to earth from space flights to nearby planets will enter the atmosphere at speeds considerably greater than returning lunar vehicles (up to twice as great). With increased entry speeds, configurations that minimize the heat input change from blunt bodies to conical shapes, and minimizing heat input can be a very important consideration at such speeds. The radiative heat input predominant for blunt bodies at hyperbolic speeds is reduced or even made negligible by use of bodies with oblique bow-shock waves (cones). The convective heat input is increased, however, so optimum cones have been sought that minimize the sum of convective and radiative heat inputs for any specified set of entry conditions (ref. 1).

One attractive method of generating lift with cones is by the use of an oblique base plane (ref. 2). This modification of a cone trimmed at zero angle of incidence has the added benefit of avoiding crossflow effects that are detrimental to retaining laminar flow, a requirement for minimum total heat input. The aerodynamic characteristics for a family of such configurations are shown in reference 3. Configurations with useful volume distribution, however, appear to be limited to either low lift-drag ratios or cone angles smaller than the optimum. In the present investigation, therefore, a parametric study was undertaken to examine other arrangements for terminating cones to obtain useful lift-drag ratios while maintaining acceptable design and performance characteristics. To simplify the analysis and to illustrate

the variety of characteristics attainable, only plane surfaces were used to terminate right circular cones. Undoubtedly, more complicated terminating surfaces can be found that give more desirable characteristics.

NOTATION

- A base area of unmodified cone
- a normal distance from cone axis to intersection of terminating surface with cone base divided by base radius (fig. 1)
- b $\tan \theta \tan \delta$
- C_D drag coefficient, $\frac{\text{drag}}{q_\infty A}$
- C_L lift coefficient, $\frac{\text{lift}}{q_\infty A}$
- C_l rolling-moment coefficient, $\frac{\text{rolling moment}}{q_\infty A d}$
- C_m pitching-moment coefficient, $\frac{\text{pitching moment}}{q_\infty A d}$
- C_N normal-force coefficient, $\frac{\text{normal force}}{q_\infty A}$
- C_n yawing-moment coefficient, $\frac{\text{yawing moment}}{q_\infty A d}$
- C_p pressure coefficient
- C_X axial-force coefficient, $\frac{\text{axial force}}{q_\infty A}$
- C_Y lateral-force coefficient, $\frac{\text{lateral force}}{q_\infty A}$
- d base diameter of unmodified cone
- J parameter defined by equations (6)
- l axial length of unmodified cone
- $\frac{L}{D}$ lift-drag ratio
- p rolling angular velocity
- q pitching angular velocity
- 2

q_{∞}	free-stream dynamic pressure
r	yawing angular velocity
S	total wetted surface area of forebody
$sste$	supersonic trailing edge
V	free-stream velocity
$\frac{vol}{vol_c}$	ratio of volume to volume of unmodified cone
x	axial distance from cone apex
x_u	axial distance from cone apex to intersection of the terminating surface and the upper cone surface (sketch (c))
y	lateral distance from cone axis
z	vertical distance from cone axis
z_t	vertical distance from cone axis to intersection of the terminating surface and the cone base (sketch (c))
α	angle of attack
β	angle of sideslip
δ	angle of terminating surface measured from the vertical (fig. 1)
θ	half-angle of cone
ω	cylindrical coordinate of cone, $\sin^{-1} \left(\frac{z}{x \tan \theta} \right)$, (sketch (a))
ω_1	cylindrical coordinate at intersection of terminating surface and cone surface (sketch (c))

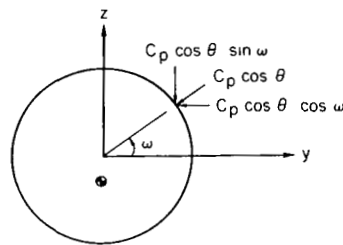
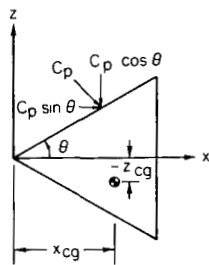
Subscripts

o	coefficient calculated for $x_{cg} = z_{cg} = 0$
cg	center of gravity
cv	center of volume
p	partial derivative with respect to $\frac{pd}{V}$ as $p \rightarrow 0$ and $\alpha = \beta = q = r = 0$

- q partial derivative with respect to $\frac{qd}{V}$ as $q \rightarrow 0$ and $\alpha = \beta = p = r = 0$
- r partial derivative with respect to $\frac{rd}{V}$ as $r \rightarrow 0$ and $\alpha = \beta = p = q = 0$
- α partial derivative with respect to α as $\alpha \rightarrow 0$ and $\beta = p = q = r = 0$
- β partial derivative with respect to β as $\beta \rightarrow 0$ and $\alpha = p = q = r = 0$

ANALYSIS

The coordinate system shown in sketch (a) was chosen to facilitate the integration of local pressure over the cone surface to obtain the total



forces and moments. The origin is at the cone apex, the x axis is coincident with the axis of revolution, and the coordinates y and z are measured perpendicular to the x axis. With respect to this system, the components of force have the same positive directions as the x, y, and z axes. Thus, the coefficients of force are seen to be

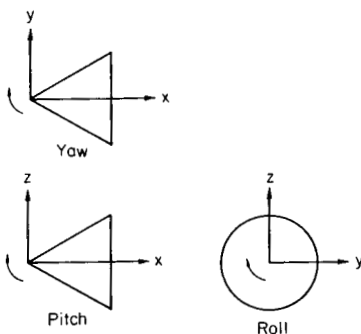
Sketch (a)

$$C_X = \frac{1}{A} \int C_p \sin \theta \, dS \quad (1a)$$

$$C_Y = - \frac{1}{A} \int C_p \cos \theta \cos \omega \, dS \quad (1b)$$

$$C_N = - \frac{1}{A} \int C_p \cos \theta \sin \omega \, dS \quad (1c)$$

where $dS = x \tan \theta \sec \theta \, d\omega \, dx$.



Sketch (b)

The sign convention chosen for the components of moment is illustrated in sketch (b) where the positive directions of the components are indicated by the arrows. Thus, the coefficients of moment about an arbitrary center-of-gravity location are

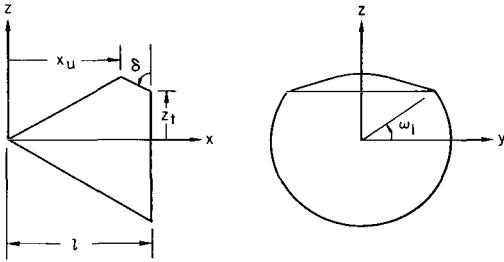
$$C_L = \frac{1}{Ad} \int z_{cg} C_p \cos \theta \cos \omega \, dS \quad (2a)$$

$$C_m = \frac{1}{Ad} \int [(x \sec^2 \theta - x_{cg}) C_p \cos \theta \sin \omega - z_{cg} C_p \sin \theta] dS \quad (2b)$$

$$C_n = \frac{1}{Ad} \int (x \sec^2 \theta - x_{cg}) C_p \cos \theta \cos \omega \, dS \quad (2c)$$

The components of angular velocity, p , q , and r , have the same positive directions as the components of moment, respectively. In addition, α is positive when the cone is at positive pitch and β is positive when the cone is at negative yaw.

Equations (2) have been written for the center of application of the resultant force located on the x axis. This center of force corresponds to the center of pressure for a symmetric body. For the present case of an unsymmetrical, cutoff cone in which the center of pressure is not on the x axis, the center of application of the resultant force is defined as the point where the resultant force intersects the x axis. The moment arms are defined relative to this point of application in the use of equations (2).



Sketch (c)

The basic assumption of Newtonian impact theory is that the flow, upon striking the body, loses its component of momentum normal to the surface, and only those portions of the body under direct impact from the stream will experience a pressure force. If the cone is terminated by a plane at an angle, δ , from the vertical (sketch (c)), the integration proceeds only over that portion of the cone receiving compression flow. The pressure coefficient is assumed to be zero

on the sheltered surfaces. Thus, the coefficients of force can be evaluated by the following integrals:

$$C_X = \frac{8 \tan^2 \theta}{\pi d^2} \left(\int_0^l \int_{-\pi/2}^{\pi/2} C_p x \, d\omega \, dx - \int_{x_u}^l \int_{\omega_1}^{\pi/2} C_p x \, d\omega \, dx \right) \quad (3a)$$

$$C_Y = - \frac{4 \tan \theta}{\pi d^2} \left(2 \int_0^l \int_0^{\pi} C_p x \cos \omega \, d\omega \, dx - \int_{x_u}^l \int_{\omega_1}^{\pi-\omega_1} C_p x \cos \omega \, d\omega \, dx \right) \quad (3b)$$

$$C_N = - \frac{8 \tan \theta}{\pi d^2} \left(\int_0^l \int_{-\pi/2}^{\pi/2} C_p x \sin \omega \, d\omega \, dx - \int_{x_u}^l \int_{\omega_1}^{\pi/2} C_p x \sin \omega \, d\omega \, dx \right) \quad (3c)$$

The coefficients of moment can be evaluated by the following integrals:

$$C_l = \frac{4 \tan \theta}{\pi d^3} z_{cg} \left(2 \int_0^l \int_0^\pi C_p x \cos \omega \, d\omega \, dx - \int_{x_u}^l \int_{\omega_1}^{\pi-\omega_1} C_p x \cos \omega \, d\omega \, dx \right) \quad (4a)$$

$$C_m = \frac{8 \tan \theta}{\pi d^3 \cos^2 \theta} \left\{ \int_0^l \int_{-\pi/2}^{\pi/2} C_p x [(x - x_{cg} \cos^2 \theta) \sin \omega - z_{cg} \sin \theta \cos \theta] \, d\omega \, dx \right. \\ \left. - \int_{x_u}^l \int_{\omega_1}^{\pi/2} C_p x [(x - x_{cg} \cos^2 \theta) \sin \omega - z_{cg} \sin \theta \cos \theta] \, d\omega \, dx \right\} \quad (4b)$$

$$C_n = \frac{4 \tan \theta}{\pi d^3 \cos^2 \theta} \left[2 \int_0^l \int_0^\pi C_p x (x - x_{cg} \cos^2 \theta) \cos \omega \, d\omega \, dx \right. \\ \left. - \int_{x_u}^l \int_{\omega_1}^{\pi-\omega_1} C_p x (x - x_{cg} \cos^2 \theta) \cos \omega \, d\omega \, dx \right] \quad (4c)$$

Let $a = 2(z_t/d)$ and $b = \tan \theta \tan \delta$, then

$$x_u = \frac{d(1+ab)}{2(1+b)\tan \theta}$$

$$\omega_1 = \sin^{-1} \frac{(1+ab) - 2(x/d)\tan \theta}{2b(x/d)\tan \theta}$$

According to impact theory, the pressure coefficient is (ref. 4)

$$C_p = 2 \left\{ \sin \theta \cos \alpha \cos \beta - \cos \theta \sin \omega \sin \alpha \cos \beta + \cos \theta \cos \omega \sin \beta \right. \\ \left. - \frac{pd}{V} \left(\frac{z}{d} \right)_{cg} \cos \theta \cos \omega - \frac{rd}{V} \left[\frac{x}{d} - \left(\frac{x}{d} \right)_{cg} \cos^2 \theta \right] \sec \theta \cos \omega \right. \\ \left. - \frac{qd}{V} \left[\frac{x}{d} \sin \omega - \left(\frac{x}{d} \right)_{cg} \cos^2 \theta \sin \omega - \left(\frac{z}{d} \right)_{cg} \sin \theta \cos \theta \right] \sec \theta \right\}^2 \quad (5)$$

Let

$$J = \frac{2(1+ab)^2}{\pi(1-b^2)^{5/2}} \cos^{-1} \frac{a+b}{1+ab} \quad \text{for } b < 1 \quad (6a)$$

$$= \frac{2(1+ab)^2}{\pi(b^2-1)^{5/2}} \ln \frac{(a+b) + \sqrt{(b^2-1)(1-a^2)}}{1+ab} \quad \text{for } b > 1 \quad (6b)$$

Thus, when $\alpha = \beta = p = q = r = 0$,

$$C_X = C_D = \sin^2 \theta \left[2 - \frac{2}{\pi} \cos^{-1} a + J(1 - b^2) - \frac{2b(1 + ab)\sqrt{1 - a^2}}{\pi(1 - b^2)} \right] \quad \text{for } b \neq 1 \quad (7a)$$

$$= \sin^2 \theta \left[2 - \frac{2}{\pi} \cos^{-1} a + \frac{2(2 + a)\sqrt{1 - a^2}}{3\pi} \right] \quad \text{for } b = 1 \quad (7b)$$

$$C_{X_\alpha} = 2 \sin \theta \cos \theta \left[Jb(1 - b^2) - \frac{2b(a + b)\sqrt{1 - a^2}}{\pi(1 - b^2)} \right] \quad \text{for } b \neq 1 \quad (7c)$$

$$= 2 \sin \theta \cos \theta \left[\frac{4(1 - a)\sqrt{1 - a^2}}{3\pi} \right] \quad \text{for } b = 1 \quad (7d)$$

$$C_{X_q} = C_{X_{q_0}} - \left(\frac{x}{d} \right)_{cg} C_{X_\alpha} + 2 \left(\frac{z}{d} \right)_{cg} C_X \quad (7e)$$

The subscript 0 indicates the coefficient for $x_{cg} = z_{cg} = 0$. Thus, $C_{X_{q_0}}$ is the derivative of the axial force due to pitching about the cone apex and is given by

$$C_{X_{q_0}} = Jb(1 + ab) - \frac{2b\sqrt{1 - a^2}}{3\pi(1 - b^2)^2} \left[3(a + b)(1 + ab) + 2b(1 - a^2)(1 - b^2) \right] \quad \text{for } b \neq 1 \quad (7f)$$

$$= \frac{4(1 - a)(4 + a)\sqrt{1 - a^2}}{15\pi} \quad \text{for } b = 1 \quad (7g)$$

$$C_Y = 0 \quad (8a)$$

$$C_{Y_\beta} = -\cos^2 \theta \left[2 - \frac{2}{\pi} \cos^{-1} a - \frac{4(1+ab)^2}{\pi b^2} \cos^{-1} a + 2J \frac{(1-b^2)^2}{b^2} + \frac{2(2+3ab)\sqrt{1-a^2}}{\pi b} \right] \quad \text{for } b \neq 1 \quad (8b)$$

$$= -\cos^2 \theta \left[2 - \frac{2}{\pi} \cos^{-1} a - \frac{4(1+a)^2}{\pi} \cos^{-1} a + \frac{2(4+5a)\sqrt{1-a^2}}{\pi} \right] \quad \text{for } b = 1 \quad (8c)$$

$$C_{Y_p} = - \left(\frac{z}{d} \right)_{cg} C_{Y_\beta} \quad (8d)$$

$$C_{Y_r} = C_{Y_{r_o}} + \left(\frac{x}{d} \right)_{cg} C_{Y_\beta} \quad (8e)$$

$$C_{Y_{r_o}} = \frac{1}{3 \tan \theta} \left\{ 2 - \frac{2}{\pi} \cos^{-1} a + J(1-b^2)(1+ab) - \frac{2b\sqrt{1-a^2}}{\pi(1-b^2)} \left[(1-b^2) + (a+b)^2 \right] \right\} \quad \text{for } b \neq 1 \quad (8f)$$

$$= \frac{1}{3 \tan \theta} \left\{ 2 - \frac{2}{\pi} \cos^{-1} a + \frac{2\sqrt{1-a^2}}{3\pi} \left[3a + 2(1-a^2) \right] \right\} \quad \text{for } b = 1 \quad (8g)$$

$$C_N = C_L = \sin \theta \cos \theta \left[Jb(1-b^2) - \frac{2b(a+b)\sqrt{1-a^2}}{\pi(1-b^2)} \right] \quad \text{for } b \neq 1 \quad (9a)$$

$$= \sin \theta \cos \theta \left[\frac{4(1-a)\sqrt{1-a^2}}{3\pi} \right] \quad \text{for } b = 1 \quad (9b)$$

$$C_{N_\alpha} = \cos^2 \theta \left\{ 2 - \frac{2}{\pi} \cos^{-1} a + \frac{4(1+ab)^2}{\pi b^2} \cos^{-1} a + 2J \frac{(1-b^2)(2b^2-1)}{b^2} - \frac{2\sqrt{1-a^2}}{\pi b(1-b^2)} \left[(1-b^2)(1+ab) + (1-a^2) + (a+b)^2 \right] \right\} \quad \text{for } b \neq 1 \quad (9c)$$

$$= \cos^2 \theta \left[2 - \frac{2}{\pi} \cos^{-1} a + \frac{4}{\pi} (1+a)^2 \cos^{-1} a - \frac{2(8+13a)\sqrt{1-a^2}}{3\pi} \right] \quad \text{for } b = 1 \quad (9d)$$

$$C_{N_q} = C_{N_{q_o}} - \left(\frac{x}{d} \right)_{cg} C_{N_\alpha} + 2 \left(\frac{z}{d} \right)_{cg} C_N \quad (9e)$$

$$C_{N_{q_0}} = \frac{1}{3 \tan \theta} \left\{ 2 - \frac{2}{\pi} \cos^{-1} a + J(1 + ab)(1 + 2b^2) - \frac{2b\sqrt{1 - a^2}}{\pi(1 - b^2)^2} \left[3(1 + ab)^2 - a(a + b)(1 - b^2) \right] \right\} \quad \text{for } b \neq 1 \quad (9f)$$

$$= \frac{1}{3 \tan \theta} \left\{ 2 - \frac{2}{\pi} \cos^{-1} a + \frac{2\sqrt{1 - a^2}}{15\pi} \left[15 + 3(1 - a) - 14(1 - a^2) \right] \right\} \quad \text{for } b = 1 \quad (9g)$$

$$C_L = 0 \quad (10a)$$

$$C_{L_\beta} = - \left(\frac{z}{d} \right)_{cg} C_{Y_\beta} \quad (10b)$$

$$C_{L_p} = - \left(\frac{z}{d} \right)_{cg} C_{L_\beta} \quad (10c)$$

$$C_{L_r} = - \left(\frac{z}{d} \right)_{cg} C_{Y_r} \quad (10d)$$

$$C_m = C_{m_0} + \left(\frac{x}{d} \right)_{cg} C_L - \left(\frac{z}{d} \right)_{cg} C_D \quad (11a)$$

Recall that the subscript 0 indicates the coefficient for $x_{cg} = z_{cg} = 0$. Thus, C_{m_0} is the coefficient of pitching moment about the cone apex:

$$C_{m_0} = -J \frac{b(1 + ab)}{2} + \frac{b\sqrt{1 - a^2}}{3\pi(1 - b^2)^2} \left[2b(1 - a^2)(1 - b^2) + 3(a + b)(1 + ab) \right] \quad \text{for } b \neq 1 \quad (11b)$$

$$= - \frac{2(1 - a)(4 + a)\sqrt{1 - a^2}}{15\pi} \quad \text{for } b = 1 \quad (11c)$$

$$C_{m_\alpha} = C_{m_{\alpha_0}} + \left(\frac{x}{d} \right)_{cg} C_{N_\alpha} - \left(\frac{z}{d} \right)_{cg} C_{X_\alpha} \quad (12a)$$

$$C_{m\alpha_0} = -\frac{1}{3 \tan \theta} \left\{ 2 - \frac{2}{\pi} \cos^{-1} a + J(1+ab)(1+2b^2) - \frac{2b\sqrt{1-a^2}}{\pi(1-b^2)^2} \left[3(1+ab)^2 - a(a+b)(1-b^2) \right] \right\} \quad \text{for } b \neq 1 \quad (12b)$$

$$= -\frac{1}{3 \tan \theta} \left\{ 2 - \frac{2}{\pi} \cos^{-1} a + \frac{2\sqrt{1-a^2}}{15\pi} \left[15 + 3(1-a) - 14(1-a^2) \right] \right\} \quad \text{for } b = 1 \quad (12c)$$

$$C_{m_q} = C_{m_{q_0}} + \left(\frac{x}{d}\right)_{cg} (C_{N_q} + C_{N_{q_0}}) - \left(\frac{z}{d}\right)_{cg} (C_{X_q} + C_{X_{q_0}}) \quad (12d)$$

$$C_{m_{q_0}} = -\frac{1}{8 \sin^2 \theta} \left\{ 2 - \frac{2}{\pi} \cos^{-1} a + J \frac{(1+4b^2)(1+ab)^2}{(1-b^2)} - \frac{2b\sqrt{1-a^2}}{3\pi(1-b^2)^3} \left[3(3+2b^2)(1+ab)^3 + 3(1-b^2)(1+ab)^2 - 3a(a+b)(1-b^2)^2 + (1-a^2)(1-b^2)(1+ab) \right] \right\} \quad \text{for } b \neq 1 \quad (12e)$$

$$= -\frac{1}{8 \sin^2 \theta} \left\{ 2 - \frac{2}{\pi} \cos^{-1} a + \frac{2\sqrt{1-a^2}}{105\pi} \left[105 + 15(1-a) - 130(1-a^2) + 26(1-a)(1-a^2) \right] \right\} \quad \text{for } b = 1 \quad (12f)$$

$$C_n = 0 \quad (13a)$$

$$C_{n\beta} = C_{n\beta_0} + \left(\frac{x}{d}\right)_{cg} C_{Y\beta} \quad (13b)$$

$$C_{n_{\beta_0}} = \frac{1}{3 \tan \theta} \left\{ 2 - \frac{2}{\pi} \cos^{-1} a + J(1 - b^2)(1 + ab) \right. \\ \left. - \frac{2b\sqrt{1 - a^2}}{\pi(1 - b^2)} \left[(1 - b^2) + (a + b)^2 \right] \right\} \quad \text{for } b \neq 1 \quad (13c)$$

$$= \frac{1}{3 \tan \theta} \left\{ 2 - \frac{2}{\pi} \cos^{-1} a + \frac{2\sqrt{1 - a^2}}{3\pi} \left[3a + 2(1 - a^2) \right] \right\} \\ \text{for } b = 1 \quad (13d)$$

$$C_{n_p} = - \left(\frac{z}{d} \right)_{cg} C_{n_\beta} \quad (13e)$$

$$C_{n_r} = C_{n_{r_0}} + \left(\frac{x}{d} \right)_{cg} (C_{Y_r} + C_{Y_{r_0}}) \quad (13f)$$

$$C_{n_{r_0}} = - \frac{1}{8 \sin^2 \theta} \left\{ 2 - \frac{2}{\pi} \cos^{-1} a + J(1 + ab)^2 \right. \\ \left. - \frac{2b\sqrt{1 - a^2}}{3\pi(1 - b^2)^2} \left[3(1 + ab)^3 + (5 + a^2)(1 - b^2)(1 + ab) \right. \right. \\ \left. \left. - 3(1 - a^2)(1 - b^2) \right] \right\} \quad \text{for } b \neq 1 \quad (13g)$$

$$= - \frac{1}{8 \sin^2 \theta} \left\{ 2 - \frac{2}{\pi} \cos^{-1} a + \frac{2\sqrt{1 - a^2}}{15\pi} \left[15a + 10(1 - a^2) \right. \right. \\ \left. \left. - 2(1 - a)(1 - a^2) \right] \right\} \quad \text{for } b = 1 \quad (13h)$$

DISCUSSION OF RESULTS

To indicate the nature of the results obtained from these equations, numerical calculations are presented for a 30° half-angle cone. Figure 1 shows the variation of lift-drag ratio with the angle of the terminating surface, δ , for various values of a . The configurations of interest have been limited to those for which $\delta \leq 90^\circ$ (no windward-facing sections of the terminating plane) and to those that retain the apex of the cone, $b = -1/a$, when a is negative. These limitations are shown on a plot of a versus δ in

figure 2. As can be seen, those configurations for which the terminating surface intersects the base of the cone below the axis at large values of δ are immediately eliminated.

If it is desired to limit the acceptable configurations to those having lift-drag ratios greater than or equal to some lower limit, a curve of constant L/D superposed on figure 2 will quickly indicate which configurations are acceptable. Figure 3 shows that a requirement of $L/D \geq 1/2$ eliminates all those configurations with $\delta < 26^\circ$ and most of the configurations for which the terminating surface intersects the base of the cone above the axis.

If it is desired to keep the component of velocity normal to the cutoff edge supersonic to prevent induced crossflow effects, then the sweep angle of the terminating edge must be locally always greater than the Mach angle (a more stringent requirement than preserving the cone apex). If the Mach number is near 5 on the surface of the cone (ref. 5), then the Mach angle is about 12° and

$$\tan^{-1}(a \tan \theta) + \tan^{-1}(1/\tan \delta) > 12^\circ$$

which reduces to

$$a \tan \theta > \tan(\delta - 78^\circ)$$

This limitation superposed on the previous figure is shown in figure 4. The line labeled supersonic trailing edge is the line described by

$$a = \frac{\tan(\delta - 78^\circ)}{\tan \theta} \quad (14)$$

In addition, if it is desired to specify a minimum acceptable volume, this boundary can be determined from the following:

$$\frac{\text{vol}}{\text{vol}_c} = \frac{1}{2} \left\{ 2 - \frac{2}{\pi} \cos^{-1} a + J(1 - b^2)(1 + ab) - \frac{2b\sqrt{1 - a^2}}{\pi(1 - b^2)} \left[(1 - b^2) + (a + b)^2 \right] \right\} \quad \text{for } b \neq 1 \quad (15a)$$

$$= \frac{1}{2} \left\{ 2 - \frac{2}{\pi} \cos^{-1} a + \frac{2\sqrt{1 - a^2}}{3\pi} \left[3a + 2(1 - a^2) \right] \right\} \quad \text{for } b = 1 \quad (15b)$$

A limitation of configurations with volumes equal to or greater than half that of the unmodified cone is shown in figure 5, again superposed on the previous figure.

These limitations cross-plotted on figure 1 are shown in figure 6. It can be seen that the maximum L/D is about 0.9 for a 30° half-angle cone with a volume ratio of $1/2$ and supersonic trailing edges.

For a vehicle to trim at zero angle of incidence,

$$C_m = C_{m_0} + C_L \left(\frac{x}{d} \right)_{cg} - C_D \left(\frac{z}{d} \right)_{cg} = 0$$

the center of gravity must be located on the line described by

$$\left(\frac{z}{d} \right)_{cg} = \frac{C_{m_0}}{C_D} + \frac{L}{D} \left(\frac{x}{d} \right)_{cg} \quad (16)$$

This line is drawn in figure 7(a) for the particular configuration of $\delta = 60^\circ$ and $\alpha = 0$. For the vehicle to be longitudinally stable,

$$C_{m_\alpha} = C_{m_{\alpha_0}} + C_{N_\alpha} \left(\frac{x}{d} \right)_{cg} - C_{X_\alpha} \left(\frac{z}{d} \right)_{cg} < 0$$

the center of gravity must be located forward of the line described by

$$\left(\frac{x}{d} \right)_{cg} = - \frac{C_{m_{\alpha_0}}}{C_{N_\alpha}} + \frac{C_{X_\alpha}}{C_{N_\alpha}} \left(\frac{z}{d} \right)_{cg} \quad (17)$$

as indicated by the solid line in figure 7(b). For directional stability,

$$C_{n_\beta} = C_{n_{\beta_0}} + C_{Y_\beta} \left(\frac{x}{d} \right)_{cg} > 0$$

the center of gravity must be forward of $-C_{n_{\beta_0}}/C_{Y_\beta}$ as indicated by the broken line in figure 7(b). The static stability limit on the center-of-gravity location is dictated by the longitudinal stability for this case. The intersection of the line for zero angle of trim (fig. 7(a)) and the limit line for static stability (fig. 7(b)) is hereinafter called the aft cg position. In addition, of course, the center of gravity must be located within the body:

$$\left(\frac{x}{d} \right)_{cg} > \frac{-C_{m_0}/C_D}{(L/D) + \tan \theta} \quad (18)$$

The center-of-gravity location at the cone surface for zero angle of trim is hereinafter called the fore cg position. The locus of permissible center-of-gravity locations is shown by the solid line in figure 7(c). Also shown in figure 7 by the small x is the location of the center of volume:

$$\begin{aligned} \left(\frac{x}{d}\right)_{cv} &= \frac{3}{16(\text{vol}/\text{vol}_c)\tan\theta} \left\{ 2 - \frac{2}{\pi} \cos^{-1} a + J(1+ab)^2 \right. \\ &\quad - \frac{2b\sqrt{1-a^2}}{3\pi(1-b^2)^2} \left[3(1+ab)^3 + (5+a^2)(1-b^2)(1+ab) \right. \\ &\quad \left. \left. - 3(1-a^2)(1-b^2) \right] \right\} \quad \text{for } b \neq 1 \quad (19a) \end{aligned}$$

$$\begin{aligned} &= \frac{3}{16(\text{vol}/\text{vol}_c)\tan\theta} \left\{ 2 - \frac{2}{\pi} \cos^{-1} a \right. \\ &\quad \left. + \frac{2\sqrt{1-a^2}}{15\pi} \left[15a + 10(1-a^2) - 2(1-a)(1-a^2) \right] \right\} \\ &\quad \text{for } b = 1 \quad (19b) \end{aligned}$$

$$\begin{aligned} \left(\frac{z}{d}\right)_{cv} &= - \frac{3}{16(\text{vol}/\text{vol}_c)} \left\{ Jb(1+ab)^2 \right. \\ &\quad \left. - \frac{2b(a+b)\sqrt{1-a^2}}{3\pi(1-b^2)^2} \left[5(1+ab)^2 - 2(a+b)^2 \right] \right\} \\ &\quad \text{for } b \neq 1 \quad (19c) \end{aligned}$$

$$= - \frac{3}{16(\text{vol}/\text{vol}_c)} \left[\frac{16(1-a)(1-a^2)^{3/2}}{15\pi} \right] \quad \text{for } b = 1 \quad (19d)$$

Plots of the fore and aft cg positions and the center-of-volume locations are shown in figure 8 for the acceptable configurations that meet the constraints of figure 5. To show the dependence on the variable a as well as δ , lines designating the configurations with $a = 0$ are included in the figure. For the particular configuration shown in figure 7, the range of permissible values of $(x/d)_{cg}$ lies between 0.44 and 0.64 and of $(z/d)_{cg}$, between -0.25 and -0.15 with $(x/d)_{cv} = 0.61$ and $(z/d)_{cv} = -0.09$.

A measure of the relative difficulty in achieving a specific center-of-gravity location is the distance between the desired location and the center of volume (ballasting distance). The minimum ballasting distance for zero angle of trim would be the perpendicular distance from the center of volume to the line described by equation (16). For most of the configurations, however, this results in static instability, that is, the center of gravity would be aft of the aft cg position. The distance from the center of

volume to the aft cg is generally the minimum ballasting distance for the acceptable configurations. This distance is shown in figure 9 along with the ballasting distance to the fore cg position. As the center of gravity is moved forward from the aft cg location, the ballasting distance is increased, making the weight and balance problem progressively more difficult. For small static margins, the ballasting distance is about equal to the vertical displacement required (0.05d to 0.10d); but, if more stability is needed, the problem becomes more difficult as the center of gravity approaches the cone surface.

The static and dynamic stability derivatives are shown in figures 10 and 11, respectively. Values for the fore and aft cg positions are plotted to indicate the limits of the values for zero angle of trim. For illustrative purposes, the values for the particular configuration with $\delta = 60^\circ$ and $a = 0$ (fig. 7) are listed below.

cg	$C_{m\alpha}$	$C_{n\beta}$	$C_{l\beta}$	C_{mq}	C_{nr}	C_{lr}	C_{np}	C_{lp}
Aft	0	0.085	-0.173	-0.069	-0.093	0.013	0.013	-0.026
Fore	-.157	.317	-.292	-.100	-.173	.080	.080	-.074

The static stability derivatives are linear with respect to center-of-gravity position, and the dynamic stability derivatives are quadratic functions of center-of-gravity position. To show the variations of the stability derivatives with center-of-gravity position, the functions listed are plotted in figure 12. This type of plot can be composed readily for any of the acceptable configurations of figure 5 with the aid of figures 8, 10, and 11, except for the dynamic stability, which requires an intermediate point. This can be obtained from figure 13, which shows the dynamic stability for $(x/d)_{cg} = 0.55$.

It may be noted that in the equations for the aerodynamic coefficients ((7) through (13)) the cone half-angle, θ , is isolated from the brackets. Thus, the results presented here for the 30° half-angle cone can be used to determine the results for other values of θ , keeping in mind that the results would apply at a different value of δ ($b = \tan \theta \tan \delta$). For example, equation (7b) shows that for $b = 1$, $C_D = 0.356$ when $a = 0$ and $\theta = 30^\circ$ ($\delta = 60^\circ$). Now, if $\theta = 40^\circ$, $C_D = 0.356 (\sin 40/\sin 30)^2 = 0.588$. This value of C_D applies at $b = 1$, which specifies that $\delta = 50^\circ$ when $\theta = 40^\circ$. A plot of L/D versus δ constructed by this method for $\theta = 40^\circ$ is shown in figure 14. The limitation of $L/D = 1/2$ can be easily applied, of course. The lines for $vol/vol_c = 1/2$ and supersonic trailing edge were constructed in the manner described above with the use of figure 6. A comparison of figures 6 and 14 shows that increasing the cone half-angle more severely limits the configurations that are acceptable and also decreases the maximum L/D .

CONCLUDING REMARKS

A parametric study was conducted to determine the aerodynamic characteristics of circular cones modified to produce lift by a cutoff plane to remove portions of the upper rearward surface. The following conclusions can be drawn from the investigation.

The Newtonian impact theory makes it possible to examine a wide range of configurations differing in cone angle, base plane angle, and volume ratio, of which previously studied cutoff cones are special cases. The aerodynamic characteristics are readily calculated as functions of the manner in which a cone is terminated at the base. The equations and curves presented provide (1) a useful means to indicate configurations that have acceptable design and stability characteristics and (2) a capability to study a large number of different vehicle shapes before resorting to wind-tunnel and free-flight tests.

The configurations studied suggest that configurations can have acceptable aerodynamic stability as well as useful lift-drag ratio and useful volume without inclining the axis of the basic cone with respect to the airstream.

Ames Research Center

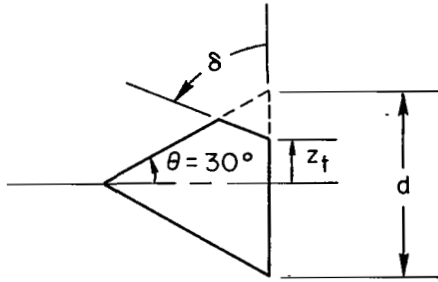
National Aeronautics and Space Administration

Moffett Field, Calif., 94035, Jan. 20, 1969

124-07-02-14-00-21

REFERENCES

1. Seiff, Alvin; and Tauber, Michael E.: Minimization of the Total Heat Input for Manned Vehicles Entering the Earth's Atmosphere at Hyperbolic Speeds. NASA TR R-236, 1966.
2. Shapland, D. J.: Preliminary Design of a Mars-Mission Earth Reentry Module. Rep. 4-57-64-3, Lockheed Missiles and Space Co., March 1964.
3. Mayo, Edward E.; Lamb, Robert H.; and Romere, Paul O.: Newtonian Aerodynamics for Blunted Raked-Off Circular Cones and Raked-Off Elliptical Cones. NASA TN D-2624, 1965.
4. Ried, Robert C., Jr.; and Mayo, Edward E.: Equations for the Newtonian Static and Dynamic Aerodynamic Coefficients for a Body of Revolution With an Offset Center-of-Gravity Location. NASA TN D-1085, 1963.
5. Romig, Mary F.: Conical Flow Parameters for Air in Dissociation Equilibrium: Final Results. Res. Note 14, Convair Scientific Research Lab., January 1958.



$$a = 2 z_f / d$$

$$b = \tan \theta \tan \delta$$

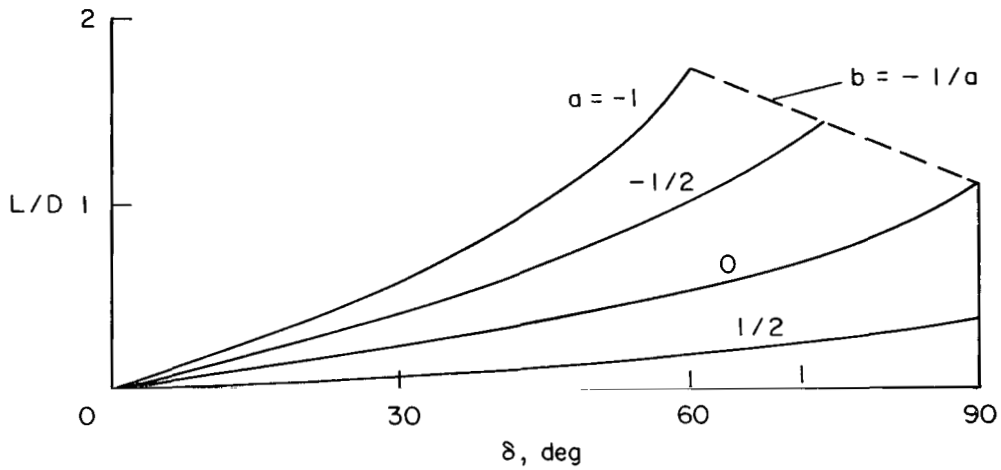


Figure 1.- Lift-drag ratios as functions of the manner in which a 30° half-angle cone is terminated.

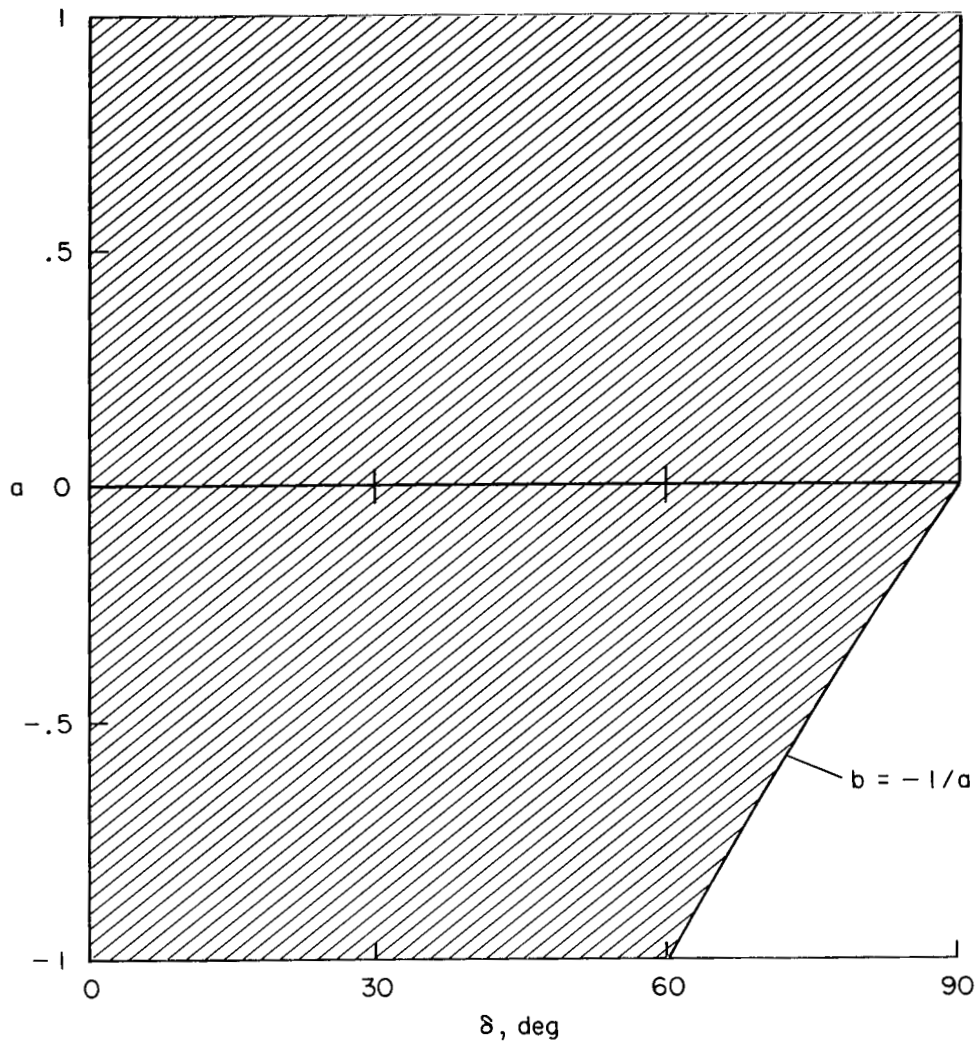


Figure 2.- Configurations that retain the cone apex, $\theta = 30^\circ$.

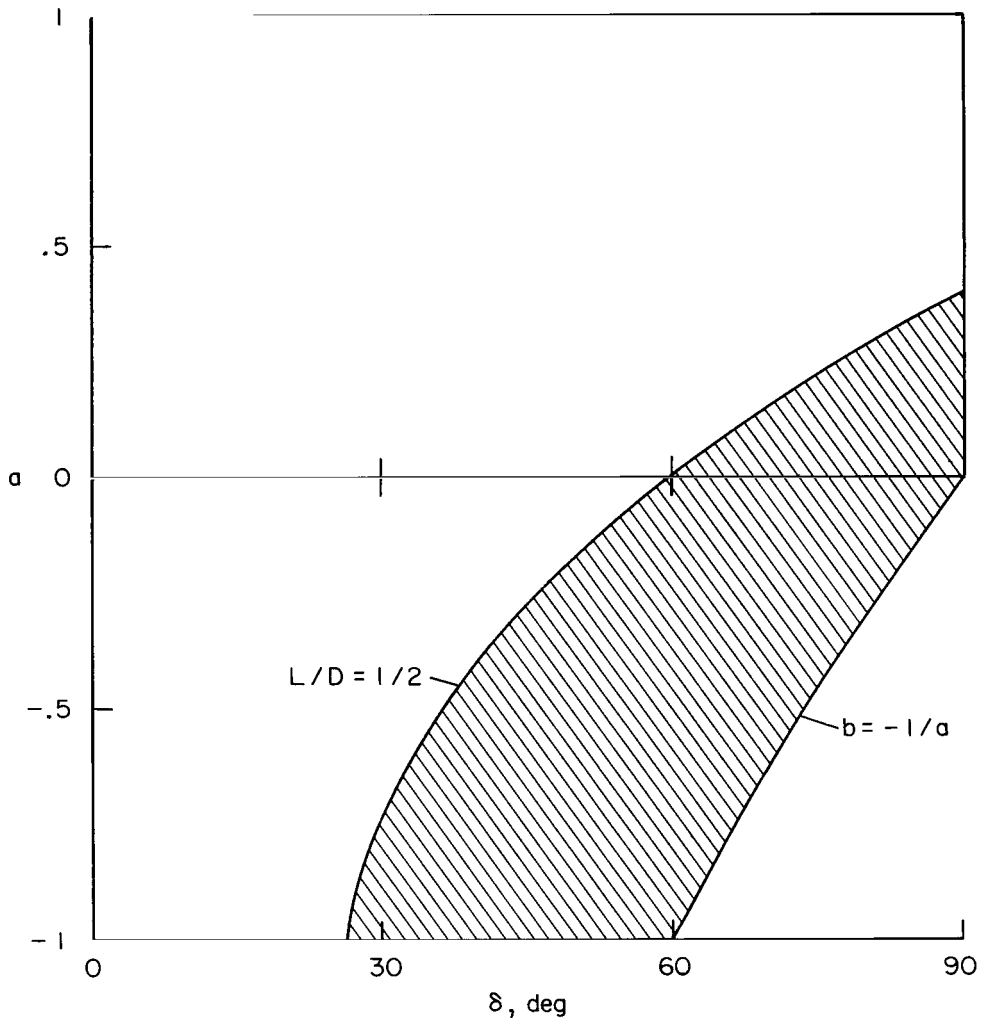


Figure 3.- Configurations with $L/D \geq 1/2$, $\theta = 30^\circ$.

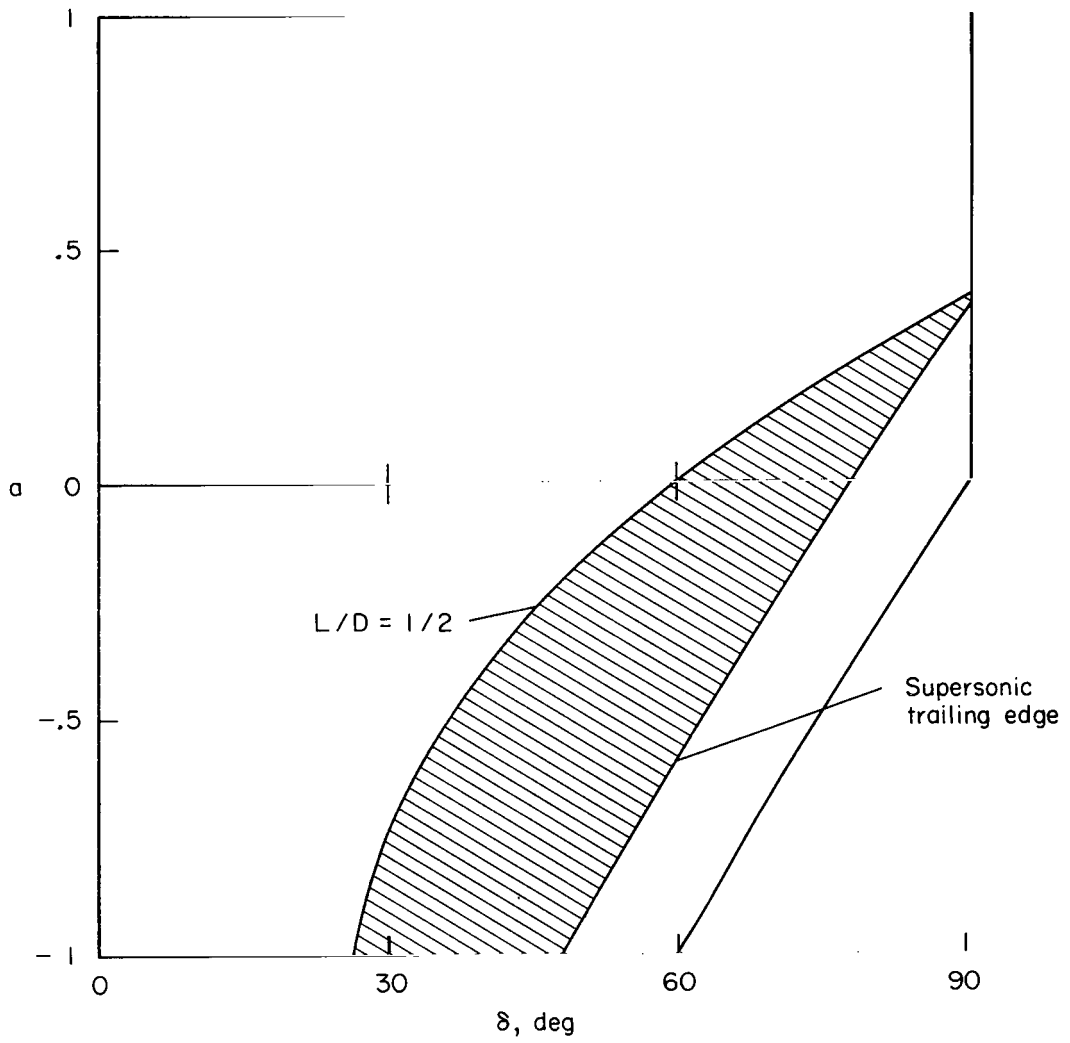


Figure 4.- Configurations with $L/D \geq 1/2$ and supersonic trailing edges, $\theta = 30^\circ$.

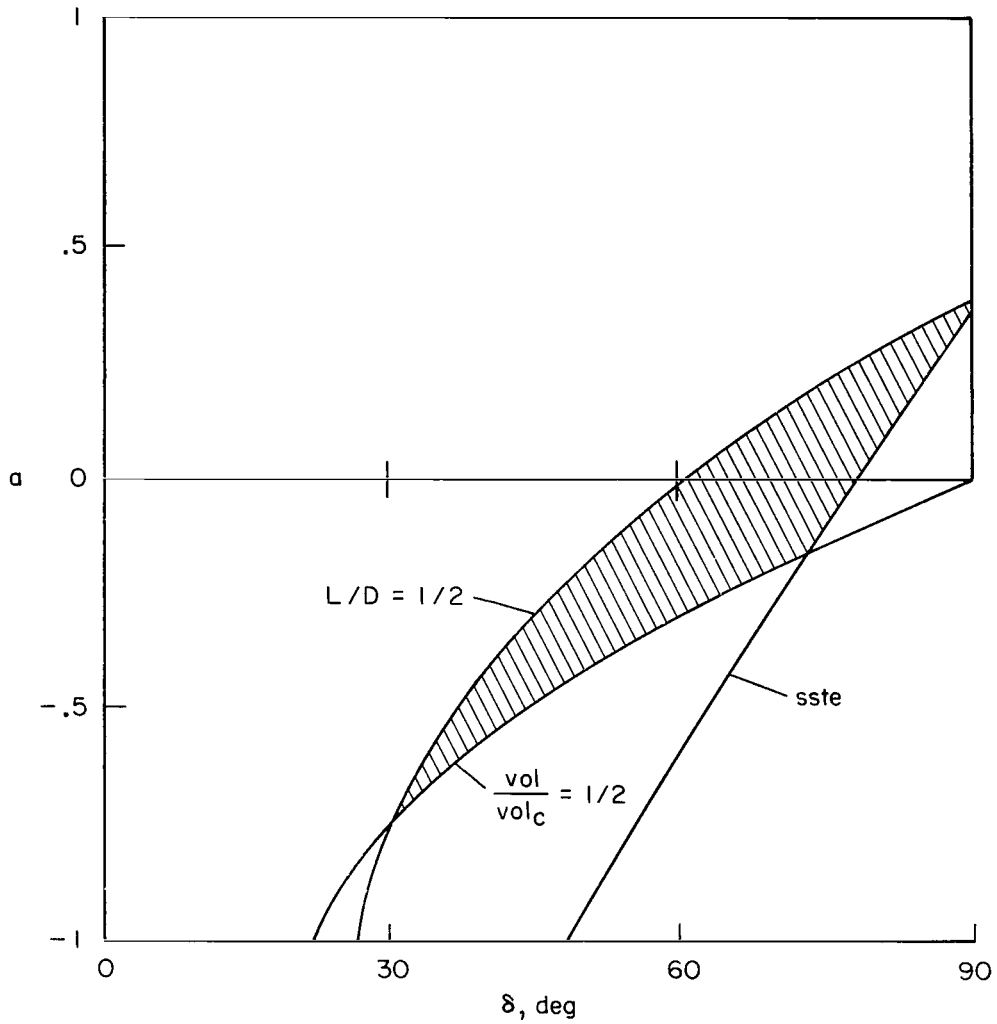


Figure 5.- Configurations with $L/D \geq 1/2$, supersonic trailing edges, and $\text{vol}/\text{vol}_c \geq 1/2$; $\theta = 30^\circ$.

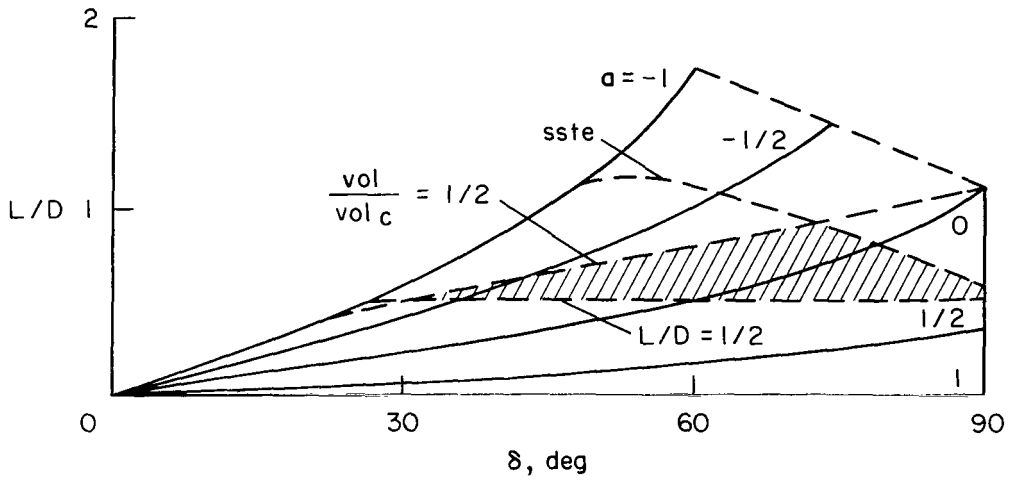
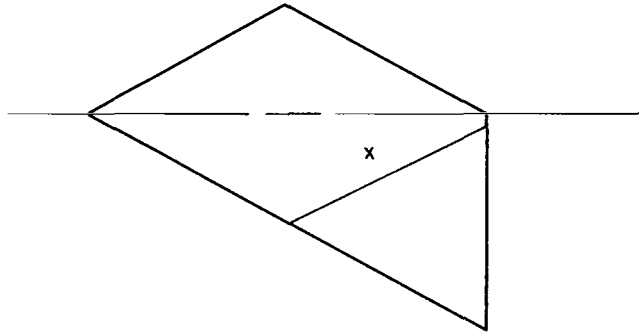
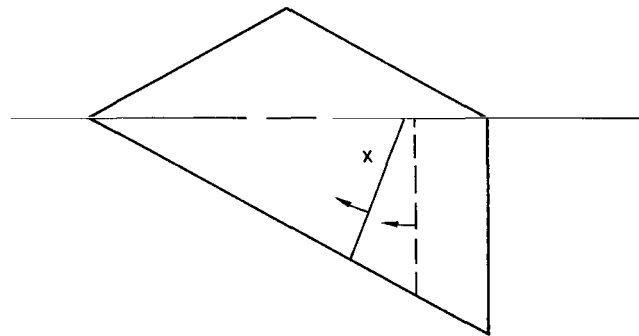


Figure 6.- Lift-drag ratios for acceptable configurations of figure 5, $\theta = 30^\circ$.

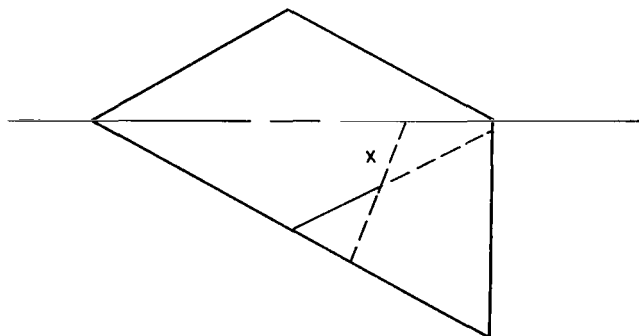
x Center of volume



(a) $C_m = 0$



(b) $C_{m_\alpha} = 0, C_{n_\beta} = 0$



(c) Statically stable at zero angle of trim

Figure 7.- Locus of permissible center-of-gravity locations for the configuration with $\delta = 60^\circ$ and $a = 0, \theta = 30^\circ$.

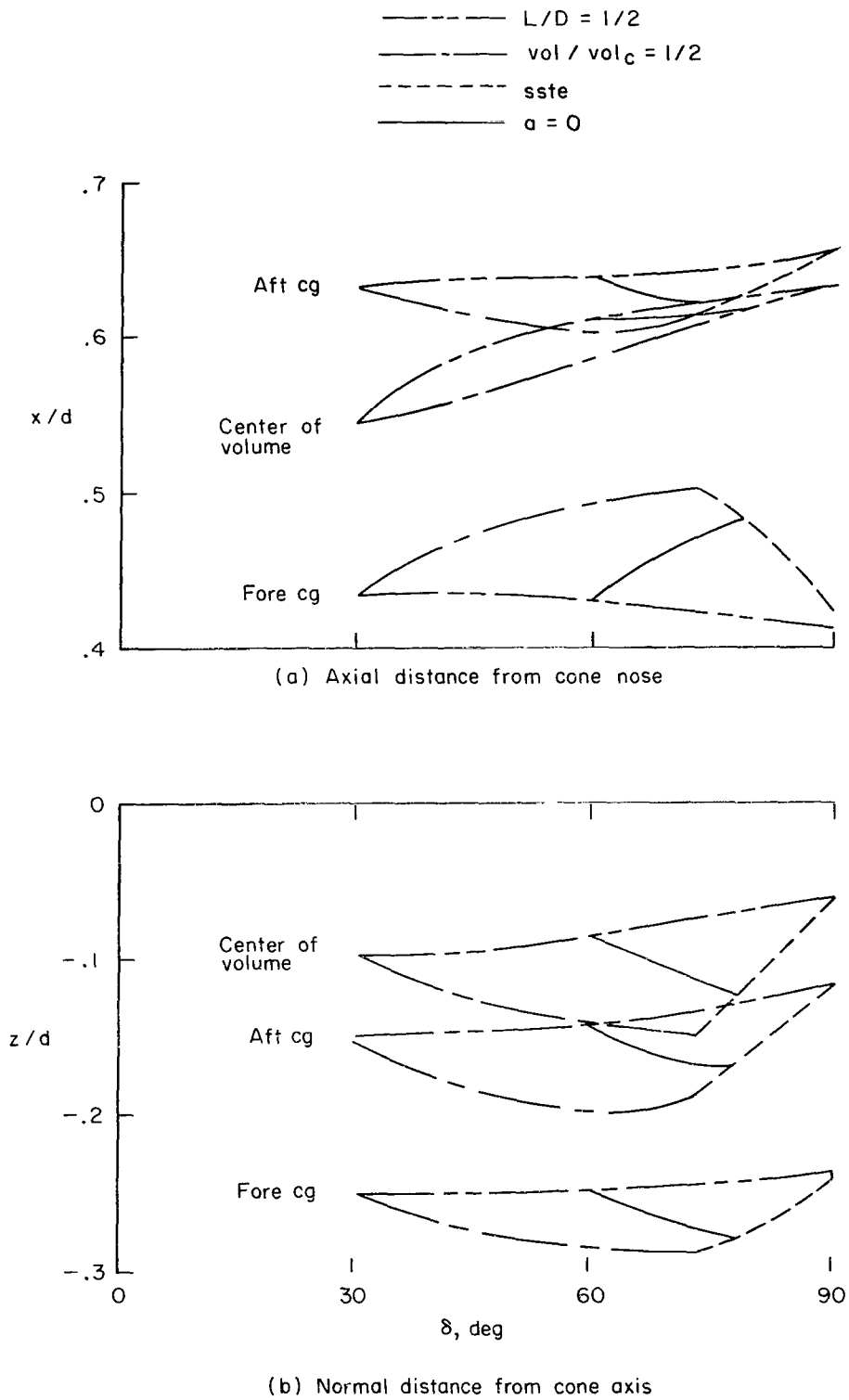


Figure 8.- Center-of-gravity and center-of-volume locations of acceptable configurations of figure 5, $\theta = 30^\circ$.

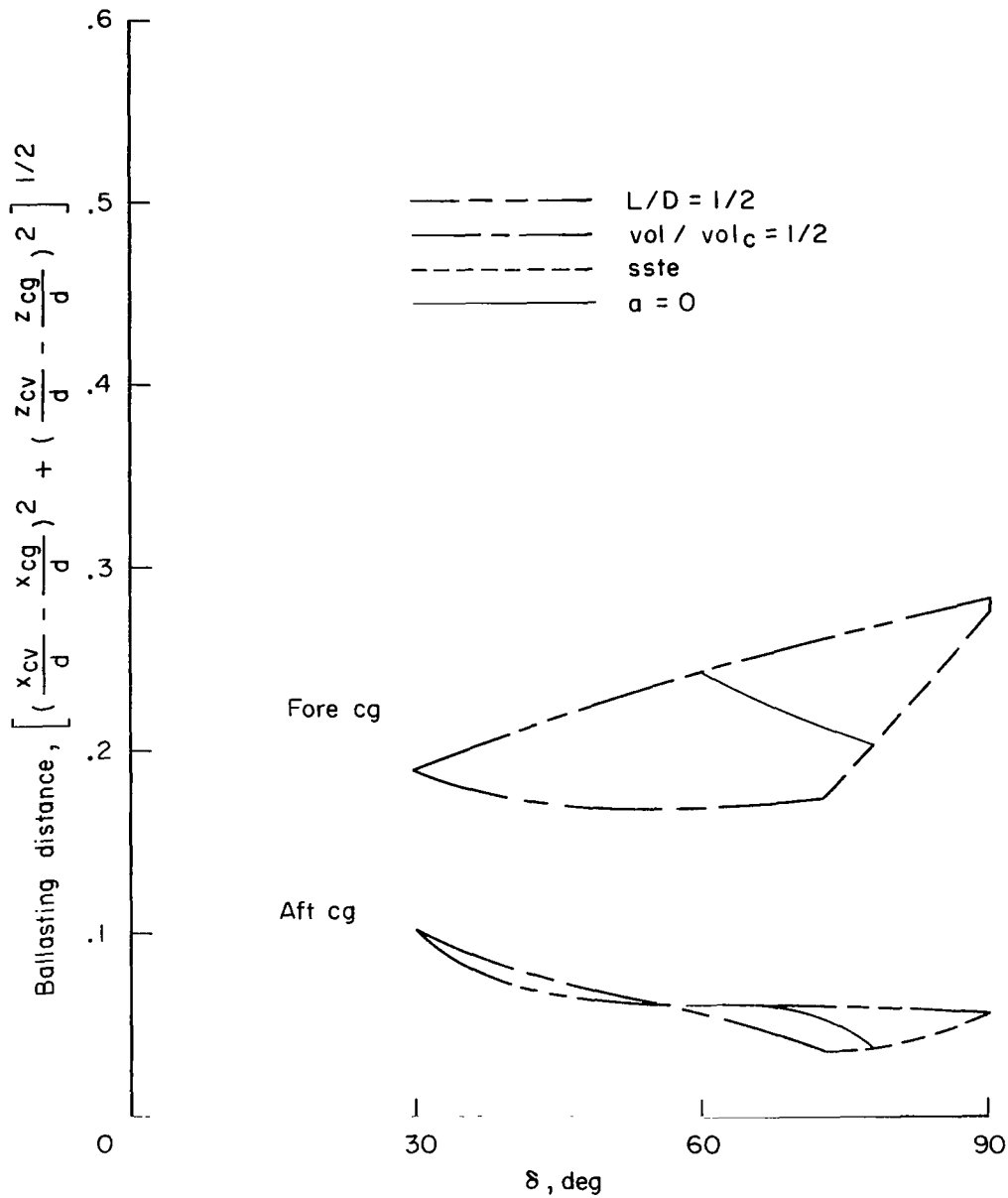
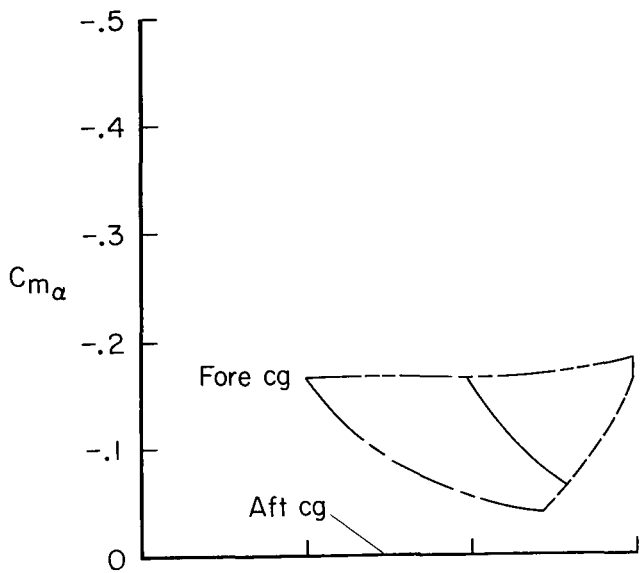
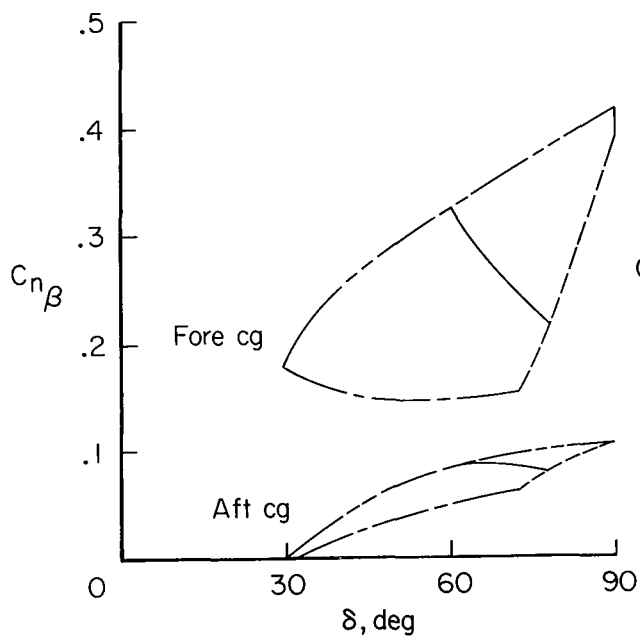


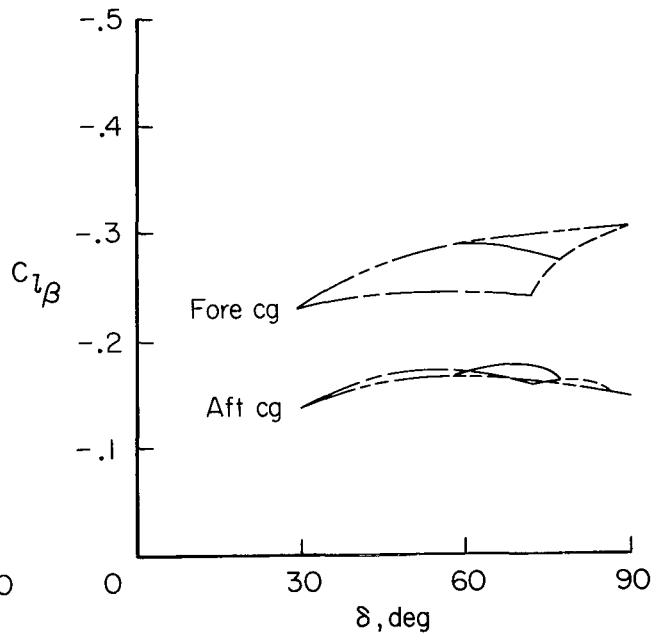
Figure 9.- Distance from center of volume to center of gravity for acceptable configurations of figure 5, $\theta = 30^\circ$.



(a) Derivative of pitching moment due to angle of attack



(b) Derivative of yawing moment due to angle of sideslip



(c) Derivative of rolling moment due to angle of sideslip

Figure 10.- Static stability of acceptable configurations of figure 5, zero angle of trim; $\theta = 30^\circ$.

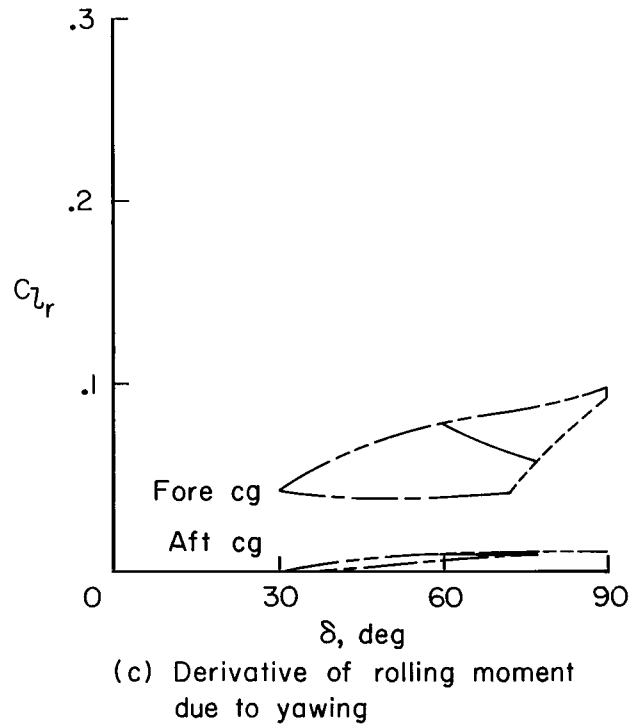
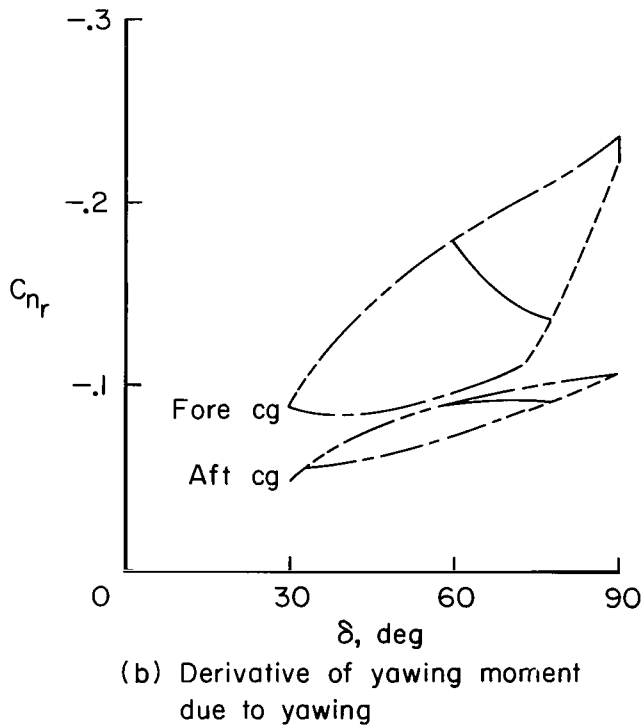
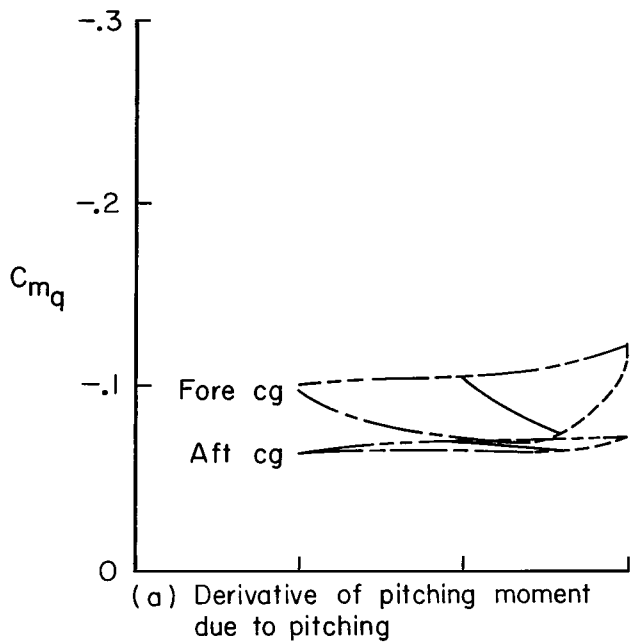


Figure 11.- Dynamic stability of acceptable configurations of figure 5, zero angle of trim; $\theta = 30^\circ$.

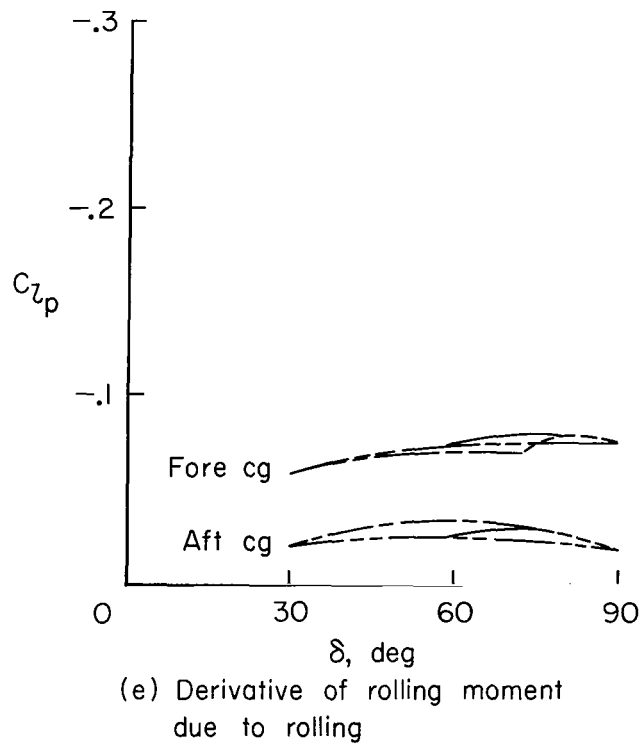
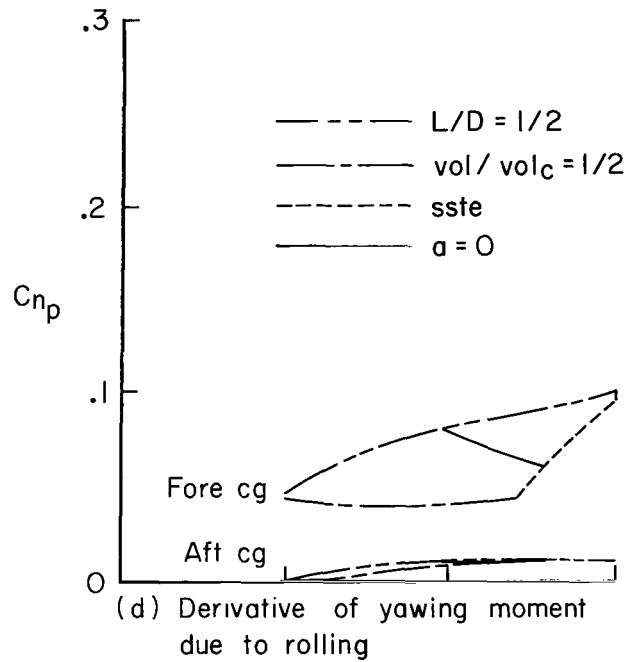


Figure 11.- Concluded.

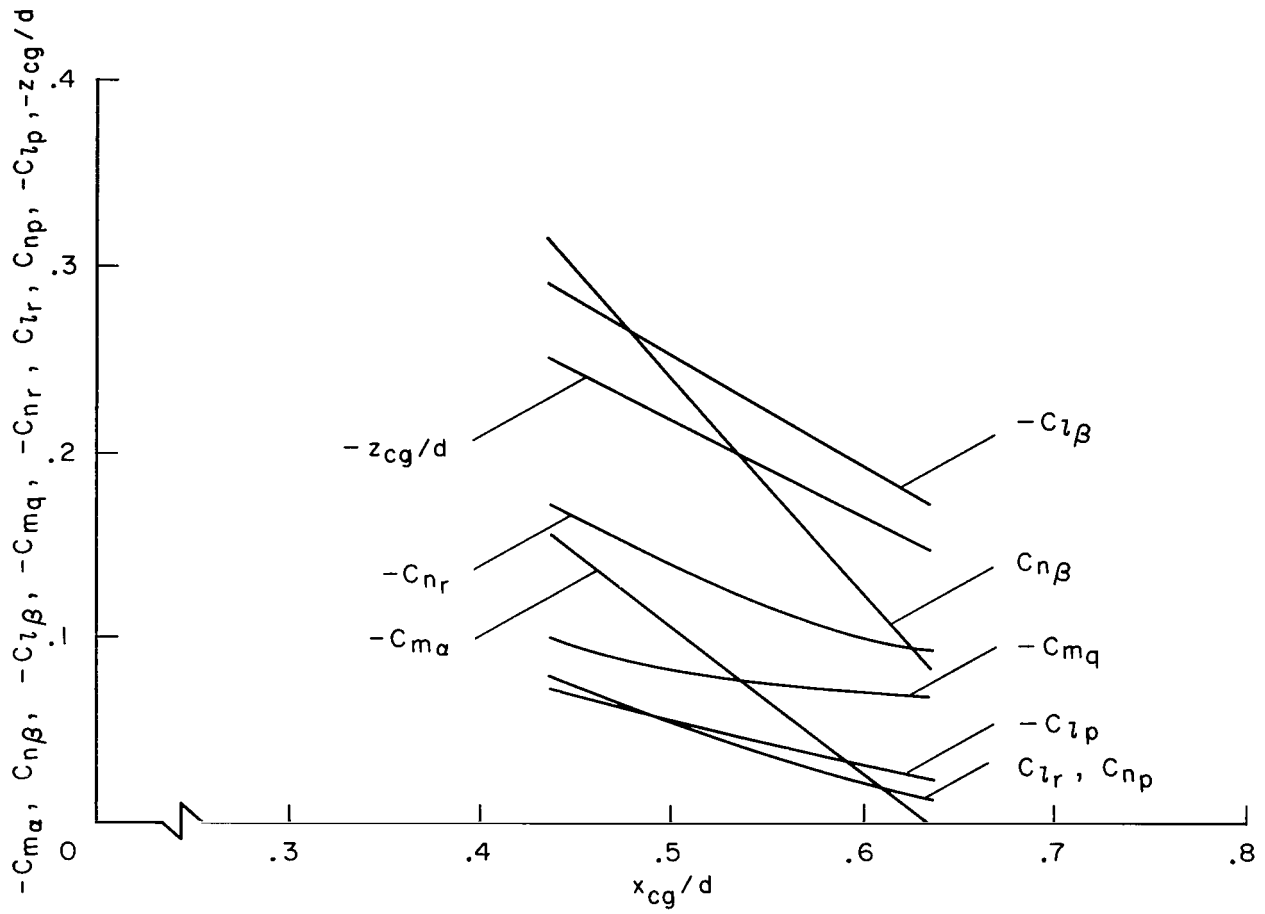


Figure 12.- Variations of stability derivatives with center-of-gravity position for the configuration with $\delta = 60^\circ$ and $\alpha = 0, \theta = 30^\circ$.

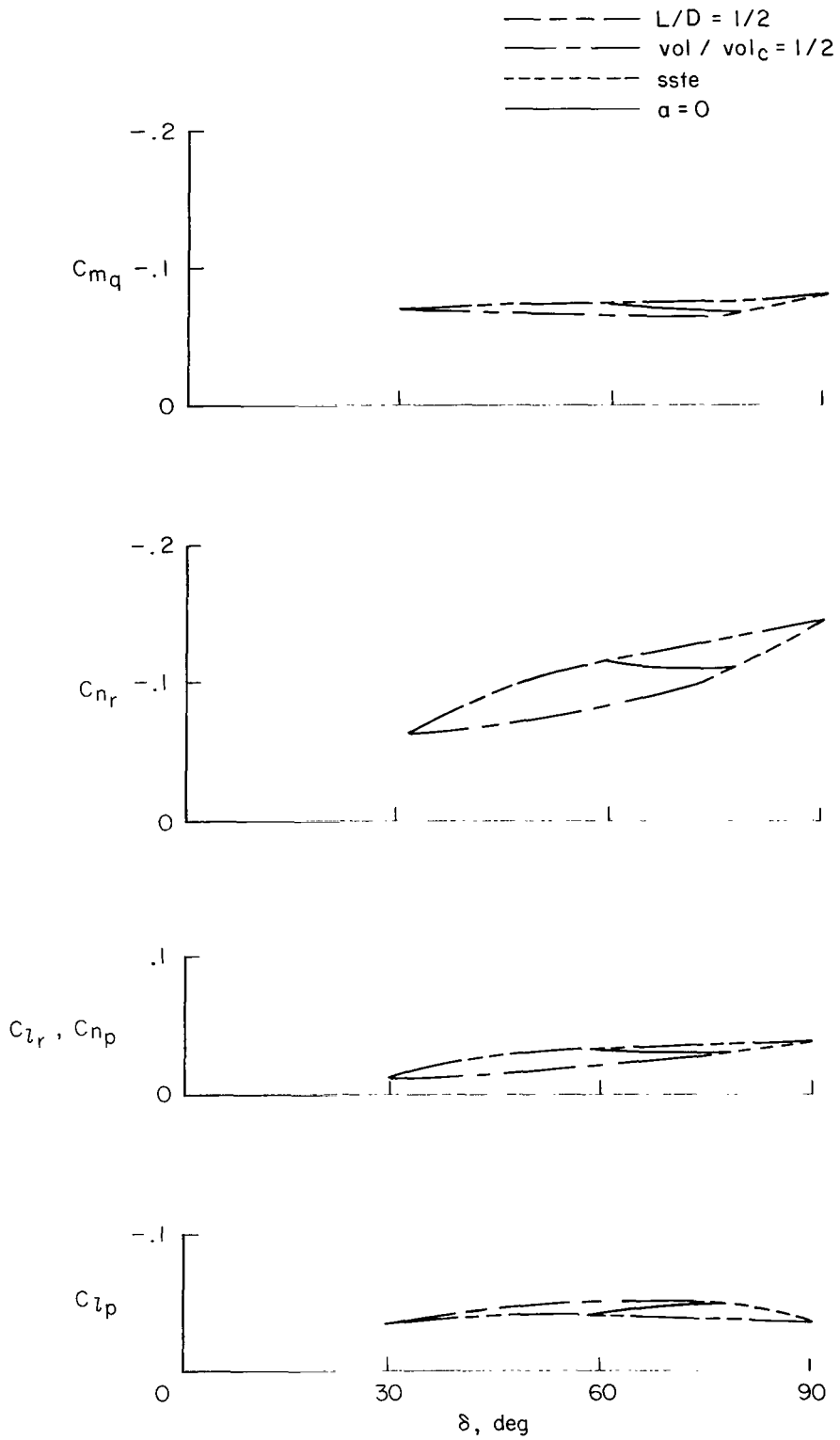


Figure 13.- Dynamic stability for acceptable configurations of figure 5, $x_{cg}/d = 0.55$; $\theta = 30^\circ$.

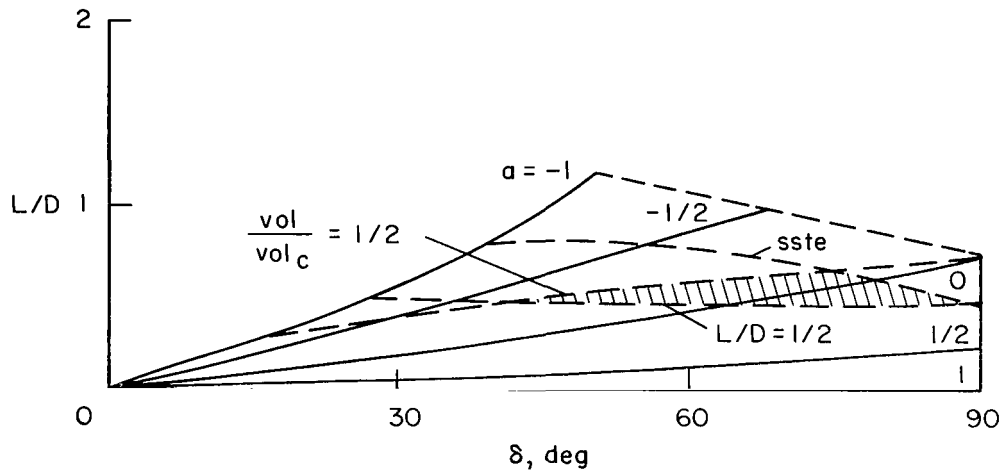


Figure 14.- Lift-drag ratios for acceptable configurations, $\theta = 40^\circ$.

FIRST CLASS MAIL

POSTMASTER: If Undeliverable (Section 1103
Postal Manual) Do Not Return

POSTMASTER: If Undeliverable (Section 1103
Postal Manual) Do Not Return

"The aeronautical and space activities of the United States shall be conducted so as to contribute . . . to the expansion of human knowledge of phenomena in the atmosphere and space. The Administration shall provide for the widest practicable and appropriate dissemination of information concerning its activities and the results thereof."

— NATIONAL AERONAUTICS AND SPACE ACT OF 1958

NASA SCIENTIFIC AND TECHNICAL PUBLICATIONS

TECHNICAL REPORTS: Scientific and technical information considered important, complete, and a lasting contribution to existing knowledge.

TECHNICAL NOTES: Information less broad in scope but nevertheless of importance as a contribution to existing knowledge.

TECHNICAL MEMORANDUMS: Information receiving limited distribution because of preliminary data, security classification, or other reasons.

CONTRACTOR REPORTS: Scientific and technical information generated under a NASA contract or grant and considered an important contribution to existing knowledge.

TECHNICAL TRANSLATIONS: Information published in a foreign language considered to merit NASA distribution in English.

SPECIAL PUBLICATIONS: Information derived from or of value to NASA activities. Publications include conference proceedings, monographs, data compilations, handbooks, sourcebooks, and special bibliographies.

TECHNOLOGY UTILIZATION PUBLICATIONS: Information on technology used by NASA that may be of particular interest in commercial and other non-aerospace applications. Publications include Tech Briefs, Technology Utilization Reports and Notes, and Technology Surveys.

Details on the availability of these publications may be obtained from:

**SCIENTIFIC AND TECHNICAL INFORMATION DIVISION
NATIONAL AERONAUTICS AND SPACE ADMINISTRATION
Washington, D.C. 20546**